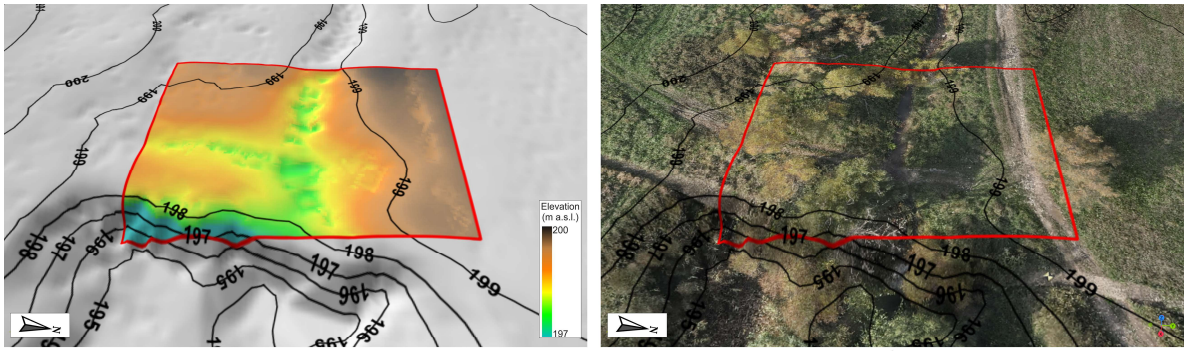

Figure S1. (a) Three-dimensional representation of a high-resolution (20 cm) Lidar-derived digital terrain model of the study area (red borders). (b) Overlay of the study area on Lidar-derived high-resolution orthophoto. Elevation is represented by black contour lines.

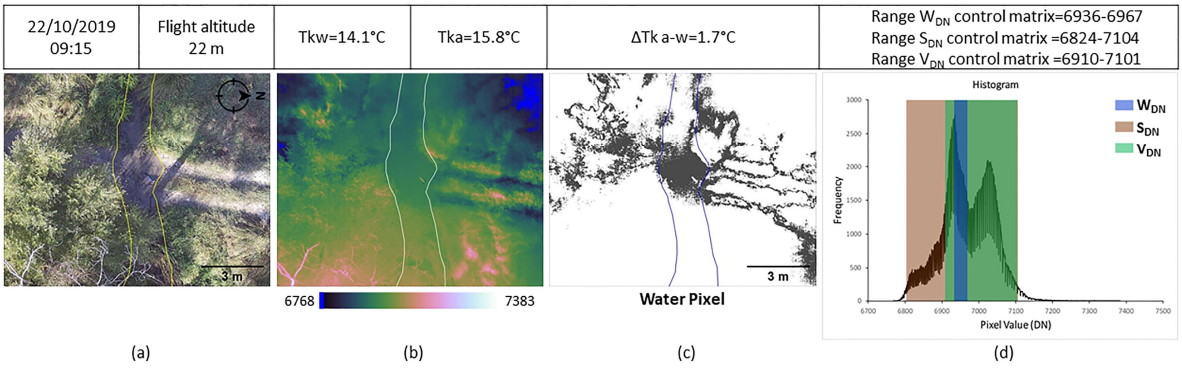

Figure S2. Surveys performed on 22 October 2019 at 09:15, 22 m flight altitude, the following images are shown: RGB image, with the delimitation of the geomorphic channel (**a**); the corresponding IR thermal image in false color, with the delimitation of the geomorphic channel (**b**); the pixels within the WDN range (**c**); the frequency distributions of the DN values of the thermal images, with three bands highlighting the WDN, SDN, and VDN ranges (**d**). Furthermore, information is provided about the date, time, and height of the flight; Tka, Tkw, and ΔTk a–w; and minimum and maximum values of the WDN, SDN, and VDN ranges.

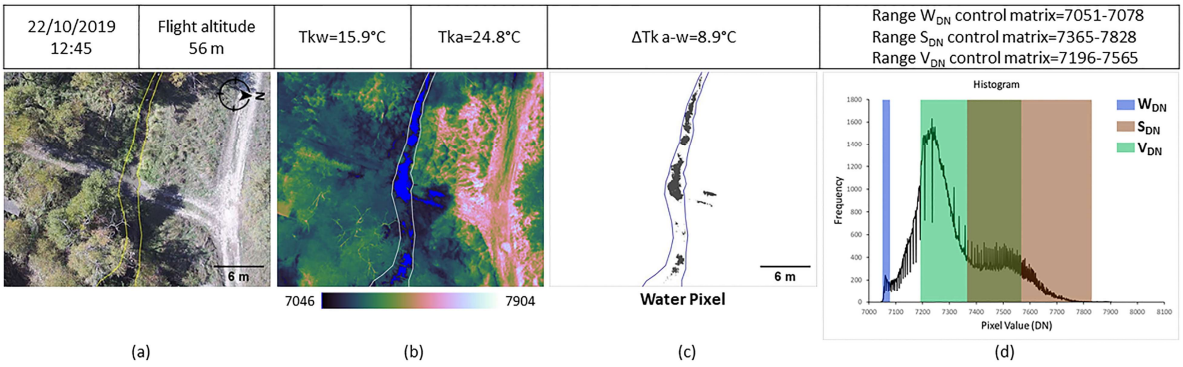

Figure S3. Surveys performed on 22 October 2019 at 12:45, 56 m flight altitude, the following images are shown: RGB image, with the delimitation of the geomorphic channel (**a**); the corresponding IR thermal image in false color, with the delimitation of the geomorphic channel (**b**); the pixels within the WDN range (**c**); the frequency distributions of the DN values of the thermal

images, with three bands highlighting the WDN, SDN, and VDN ranges (**d**). Furthermore, information is provided about the date, time, and height of the flight; Tka, Tkw, and ΔTk a–w; and minimum and maximum values of the WDN, SDN, and VDN ranges.

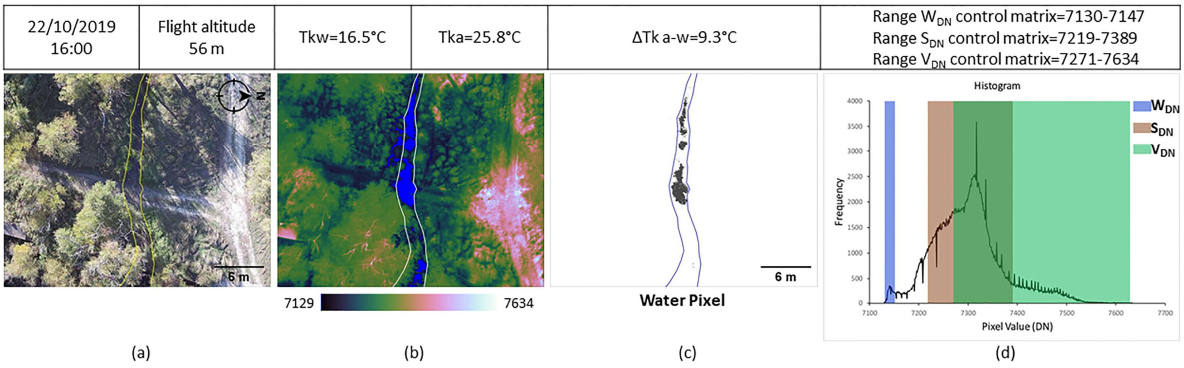

Figure S4. Surveys performed on 22 October 2019 at 16:00, 56 m flight altitude, the following images are shown: RGB image, with the delimitation of the geomorphic channel (**a**); the corresponding IR thermal image in false color, with the delimitation of the geomorphic channel (**b**); the pixels within the WDN range (**c**); the frequency distributions of the DN values of the thermal images, with three bands highlighting the WDN, SDN, and VDN ranges (**d**). Furthermore, information is provided about the date, time, and height of the flight; Tka, Tkw, and ΔTk a–w; and minimum and maximum values of the WDN, SDN, and VDN ranges.

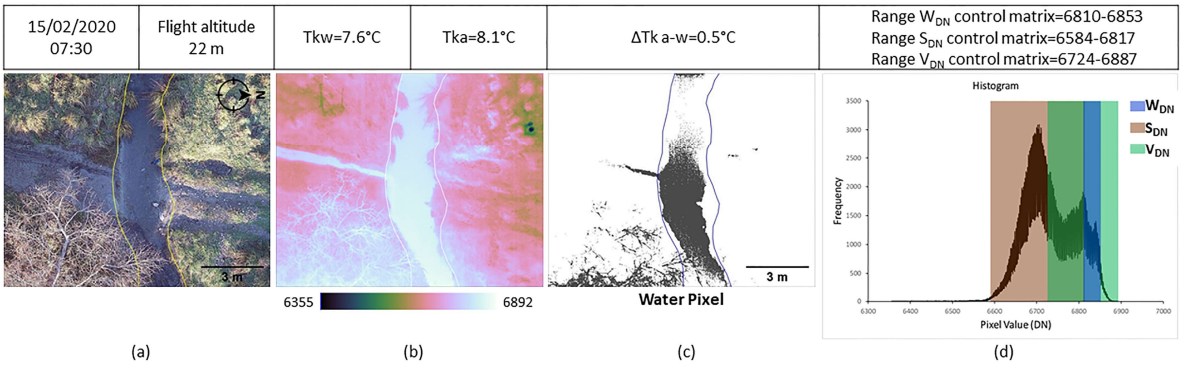

Figure S5. Surveys performed on 15 February 2020 at 07:30, 22 m flight altitude, the following images are shown: RGB image, with the delimitation of the geomorphic channel (**a**); the corresponding IR thermal image in false color, with the delimitation of the geomorphic channel (**b**); the pixels within the WDN range (**c**); the frequency distributions of the DN values of the thermal images, with three bands highlighting the WDN, SDN, and VDN ranges (**d**). Furthermore, information is provided about the date, time, and height of the flight; Tka, Tkw, and ΔTk a–w; and minimum and maximum values of the WDN, SDN, and VDN ranges.

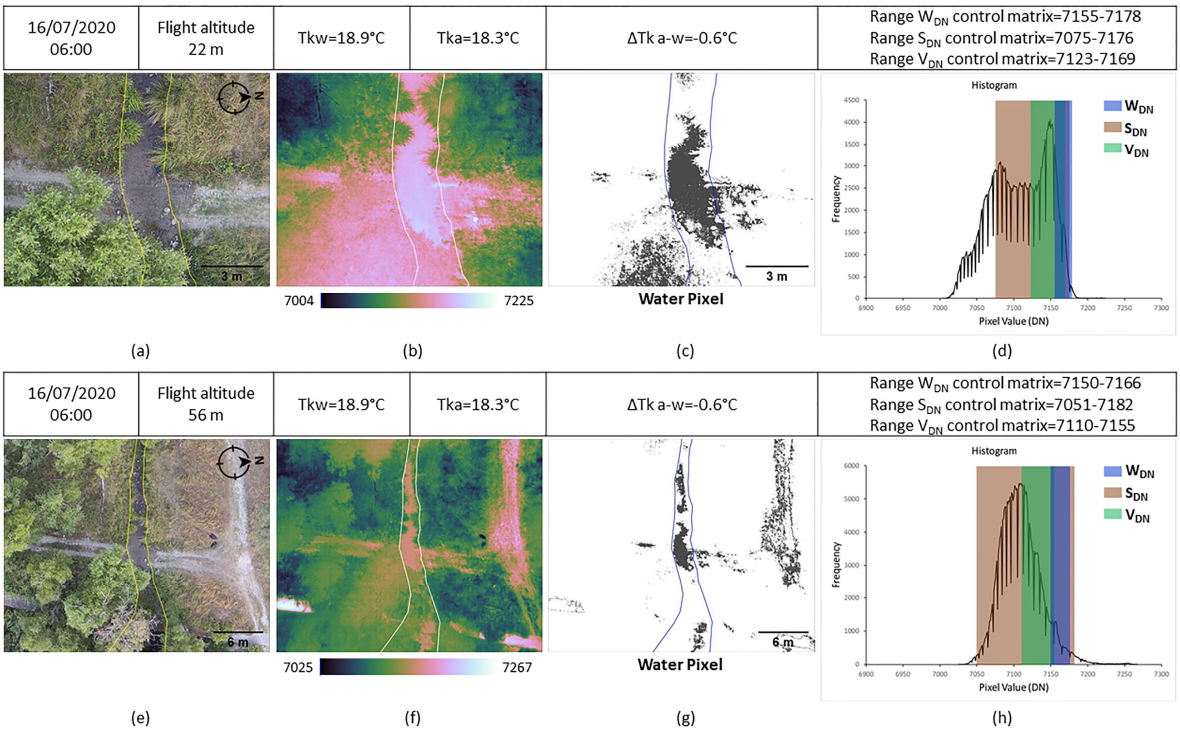

Figure S6. Surveys performed on 16 July 2020 at 06:00, 22 m and 56 m flight altitude, the following images are shown: RGB image, with the delimitation of the geomorphic channel (**a**,**e**); the corresponding IR thermal image in false color, with the delimitation of the geomorphic channel (**b**,**f**); the pixels within the WDN range (**c**,**g**); the frequency distributions of the DN values of the thermal images, with three bands highlighting the WDN, SDN, and VDN ranges (**d**,**h**). Furthermore, information is provided about the date, time, and height of the flight; Tka, Tkw, and ΔTk a–w; and minimum and maximum values of the WDN, SDN, and VDN ranges.

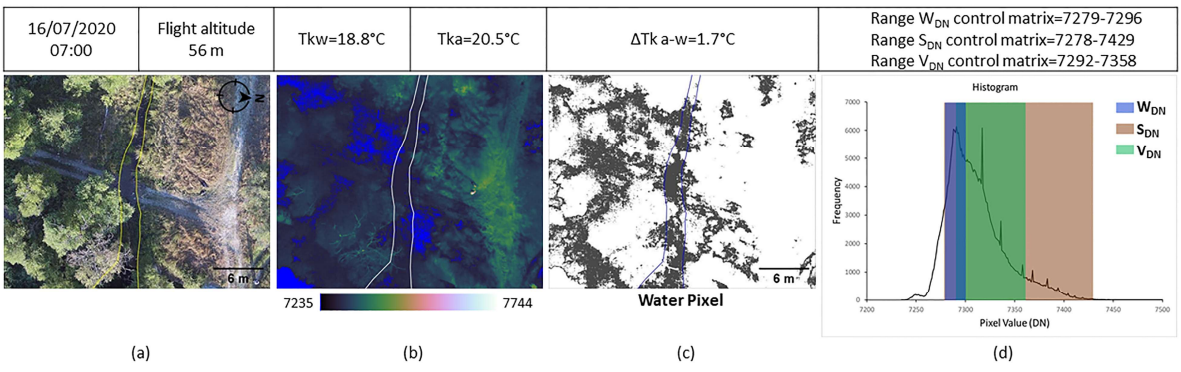

Figure S7. Surveys performed on 16 July 2020 at 07:00, 56 m flight altitude, the following images are shown: RGB image, with the delimitation of the geomorphic channel (**a**); the corresponding IR thermal image in false color, with the delimitation of the geomorphic channel (**b**); the pixels within the WDN range (**c**); the frequency distributions of the DN values of the thermal images, with three bands highlighting the WDN, SDN, and VDN ranges (**d**). Furthermore, information is provided about the date, time, and height of the flight; Tka, Tkw, and ΔTk a–w; and minimum and maximum values of the WDN, SDN, and VDN ranges.

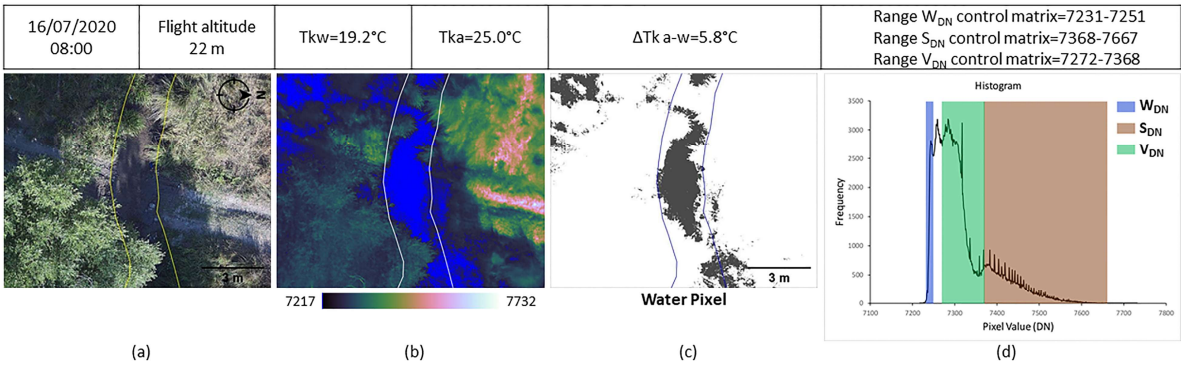

Figure S8. Surveys performed on 16 July 2020 at 08:00, 22 m flight altitude, the following images are shown: RGB image, with the delimitation of the geomorphic channel (**a**); the corresponding IR thermal image in false color, with the delimitation of the geomorphic channel (**b**); the pixels within the WDN range (**c**); the frequency distributions of the DN values of the thermal images, with three bands highlighting the WDN, SDN, and VDN ranges (**d**). Furthermore, information is provided about the date, time, and height of the flight; Tka, Tkw, and ΔTk a–w; and minimum and maximum values of the WDN, SDN, and VDN ranges.

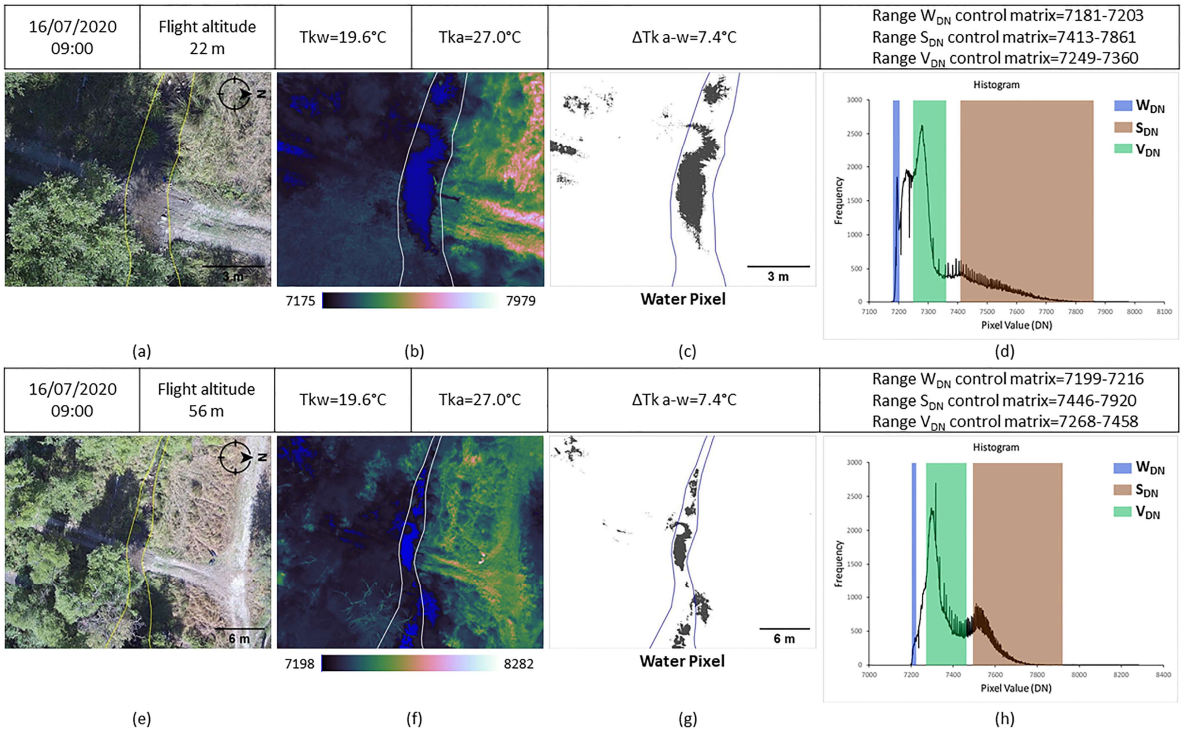

Figure S9. Surveys performed on 16 July 2020 at 09:00, 22 m and 56 m flight altitude, the following images are shown: RGB image, with the delimitation of the geomorphic channel (**a**,**e**); the corresponding IR thermal image in false color, with the delimitation of the geomorphic channel (**b**,**f**); the pixels within the WDN range (**c**,**g**); the frequency distributions of the DN values of the thermal images, with three bands highlighting the WDN, SDN, and VDN ranges (**d**,**h**). Furthermore, information is provided about the date, time, and height of the flight; Tka, Tkw, and ΔTk a–w; and minimum and maximum values of the WDN, SDN, and VDN ranges.

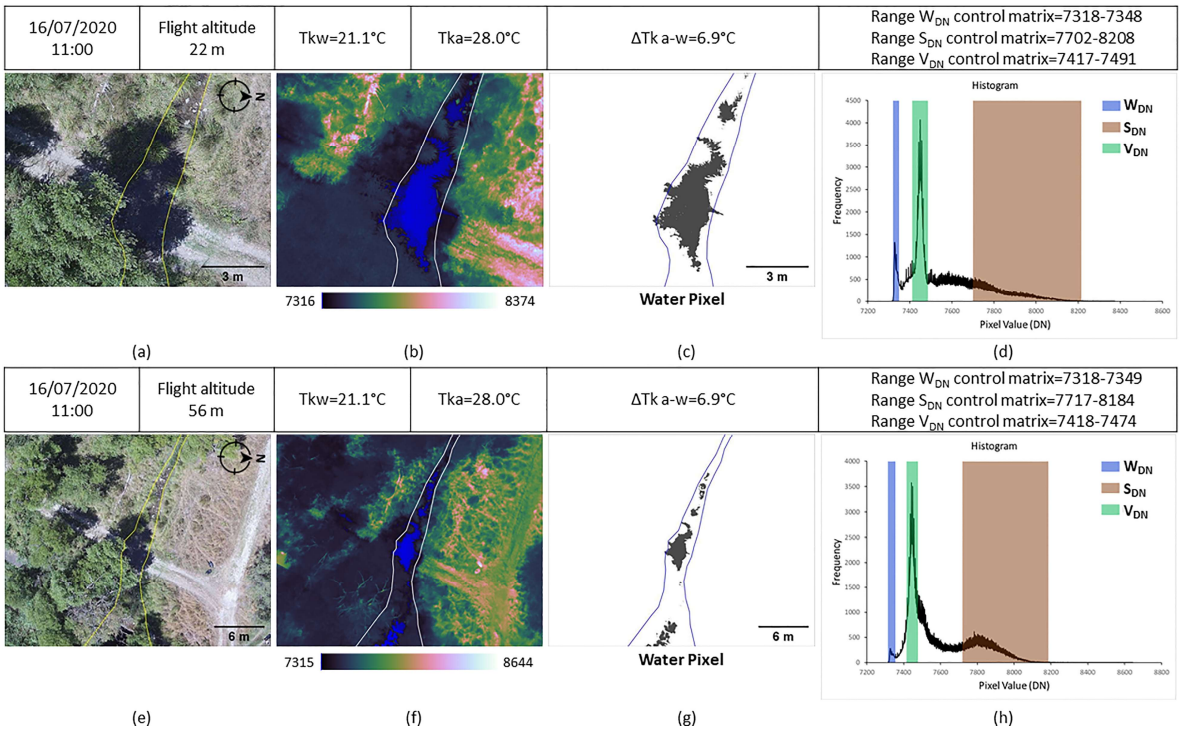

Figure S10. Surveys performed on 16 July 2020 at 11:00, 22 m and 56 m flight altitude, the following images are shown: RGB image, with the delimitation of the geomorphic channel (**a**,**e**); the corresponding IR thermal image in false color, with the delimitation of the geomorphic channel (**b**,**f**); the pixels within the WDN range (**c**,**g**); the frequency distributions of the DN values of the thermal images, with three bands highlighting the WDN, SDN, and VDN ranges (**d**,**h**). Furthermore, information is provided about the date, time, and height of the flight; Tka, Tkw, and ΔTk a–w; and minimum and maximum values of the WDN, SDN, and VDN ranges.

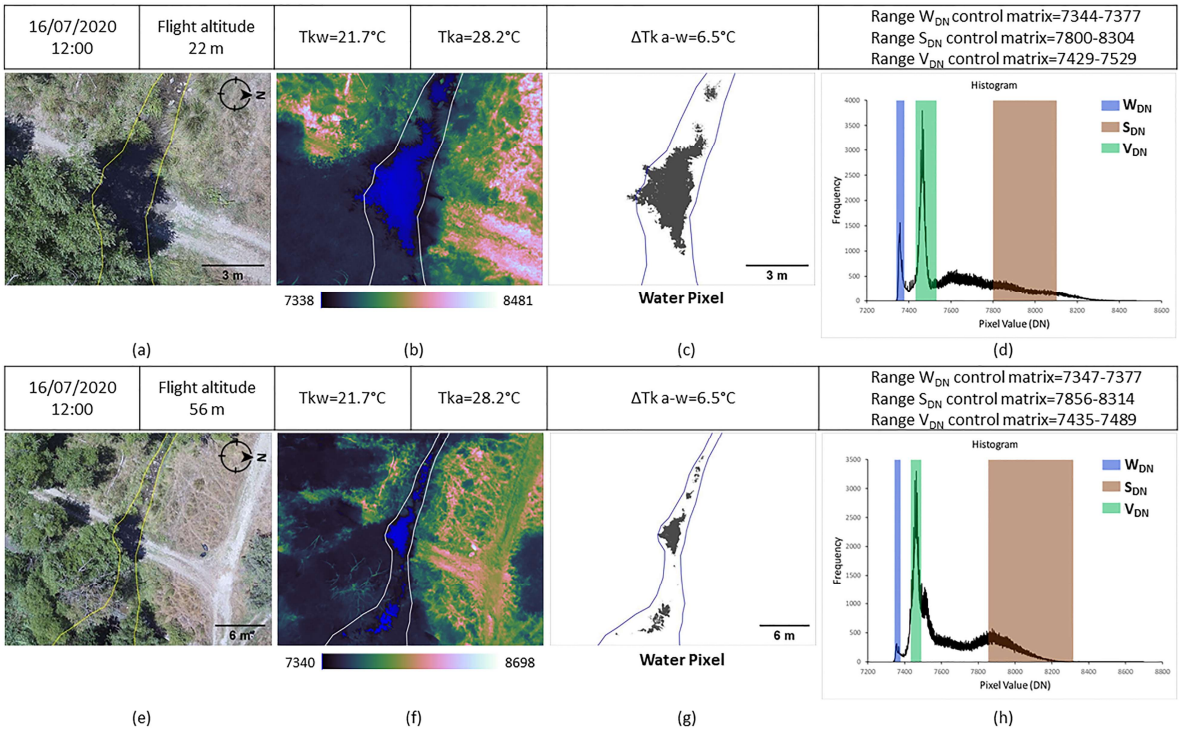

Figure S11. Surveys performed on 16 July 2020 at 12:00, 22 m and 56 m flight altitude, the following images are shown: RGB image, with the delimitation of the geomorphic channel (**a**,**e**); the

corresponding IR thermal image in false color, with the delimitation of the geomorphic channel (**b**,**f**); the pixels within the WDN range (**c**,**g**); the frequency distributions of the DN values of the thermal images, with three bands highlighting the WDN, SDN, and VDN ranges (**d**,**h**). Furthermore, information is provided about the date, time, and height of the flight; Tka, Tkw, and ΔTk a–w; and minimum and maximum values of the WDN, SDN, and VDN ranges.

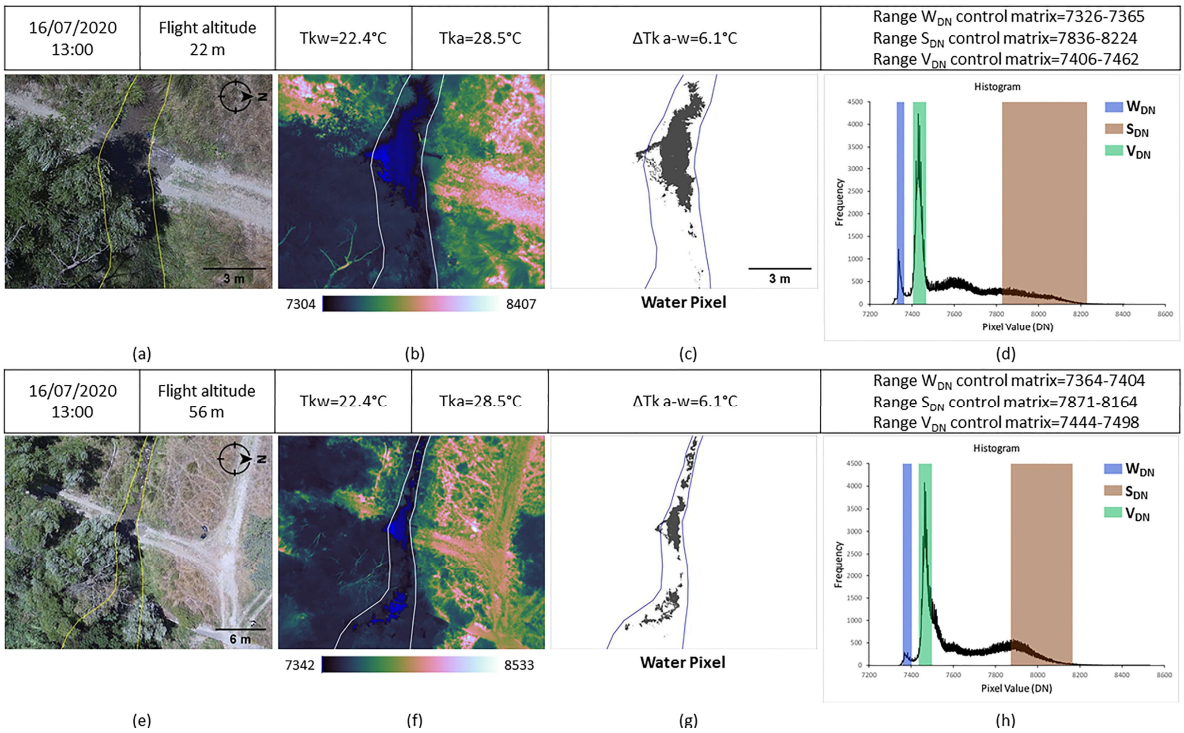

Figure S12. Surveys performed on 16 July 2020 at 13:00, 22 m and 56 m flight altitude, the following images are shown: RGB image, with the delimitation of the geomorphic channel (**a**,**e**); the corresponding IR thermal image in false color, with the delimitation of the geomorphic channel (**b**,**f**); the pixels within the WDN range (**c**,**g**); the frequency distributions of the DN values of the thermal images, with three bands highlighting the WDN, SDN, and VDN ranges (**d**,**h**). Furthermore, information is provided about the date, time, and height of the flight; Tka, Tkw, and ΔTk a–w; and minimum and maximum values of the WDN, SDN, and VDN ranges.

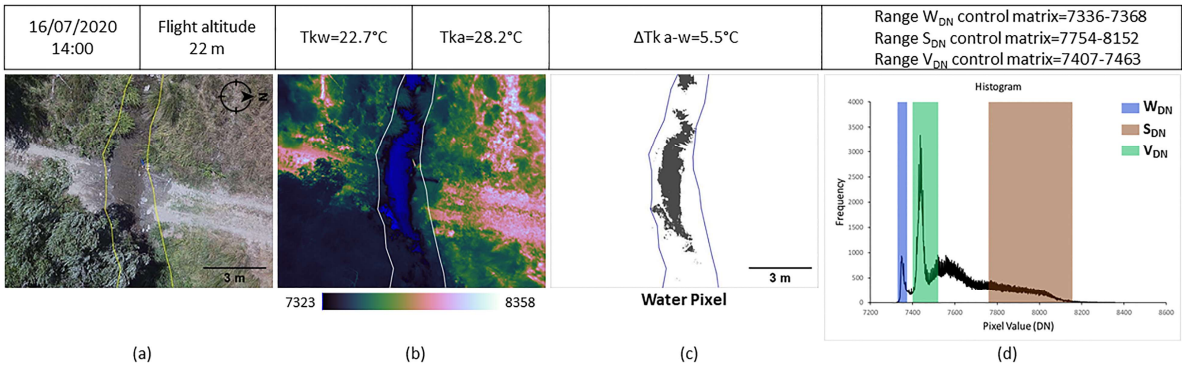

Figure S13. Surveys performed on 16 July 2020 at 16:00, 22 m flight altitude, the following images are shown: RGB image, with the delimitation of the geomorphic channel (**a**); the corresponding IR thermal image in false color, with the delimitation of the geomorphic channel (**b**); the pixels within the WDN range (**c**); the frequency distributions of the DN values of the thermal images, with three

bands highlighting the WDN, SDN, and VDN ranges (**d**). Furthermore, information is provided about the date, time, and height of the flight; Tka, Tkw, and ΔTk a–w; and minimum and maximum values of the WDN, SDN, and VDN ranges.